Molecular Therapy
Nucleic Acids
Original Article

BTEB2-Activated lncRNA TSPEAR-AS2 Drives GC Progression through Suppressing GJA1 Expression and Upregulating CLDN4 Expression

Zhong-Hua Ma,[1] You Shuai,[2] Xiang-Yu Gao,[1] Yan Yan,[3] Ke-Ming Wang,[4] Xian-Zi Wen,[1] and Jia-Fu Ji[1]

[1]Key Laboratory of Carcinogenesis and Translational Research (Ministry of Education), Division of Gastrointestinal Cancer Translational Research Laboratory, Peking University Cancer Hospital and Institute, Beijing, China; [2]Department of Medical Oncology, Jiangsu Cancer Hospital, Jiangsu Institute of Cancer Research, The Affiliated Cancer Hospital of Nanjing Medical University, Nanjing, Jiangsu, China; [3]Department of Endoscopy Center, Key Laboratory of Carcinogenesis and Translational Research (Ministry of Education), Peking University Cancer Hospital and Institute, Beijing 100142, China; [4]Department of Oncology, The Second Clinical Medical College of Nanjing Medical University, Nanjing, Jiangsu, China

Long non-coding RNAs (lncRNAs) are characterized as key layers of the genome in various cancers. TSPEAR-AS2 was highlighted to be a candidate lncRNA potentially involved in gastric cancer (GC) progression. However, the clinical significance and mechanism of TSPEAR-AS2 in GC required clarification. The clinical significance of TSPEAR-AS2 was elucidated through Kaplan-Meier Plotter. The mechanism of TSPEAR-AS2 in GC was clarified *in vitro* and *in vivo* using luciferase reporter, chromatin immunoprecipitation, RNA immunoprecipitation assays, and animal models. TSPEAR-AS2 elevation was closely correlated with overall survival of GC patients. A basic transcription element-binding protein 2 (BTEB2)-activated TSPEAR-AS2 model was first explored in this study. TSPEAR-AS2 silencing substantially reduced tumorigenic capacities of GC cells, while TSPEAR-AS2 elevation had the opposite effect. Mechanistically, TSPEAR-AS2 bound with both polycomb repressive complex 2 (PRC2) and argonaute 2 (Ago2). TSPEAR-AS2 knockdown significantly decreased H3K27me3 levels at promoter regions of gap junction protein alpha 1 (GJA1). Ago2 was recruited by TSPEAR-AS2, which was defined to sponge miR-1207-5p, contributing to the repression of claudin 4 (CLDN4) translation. The axis of EZH2/GJA1 and miR-1207-5p/CLDN4 mediated by BTEB2-activated-TSPEAR-AS2 plays an important role in GC progression, suggesting a new therapeutic direction in GC treatment.

INTRODUCTION

Gastric cancer (GC) is an important issue strongly linked to public health, ranking as the third leading cause of cancer death globally.[1] Despite tremendous progress in the clinical detection and treatment of GC in recent decades, the prognosis remains unsatisfactory, with a 5-year survival rate of less than 30% in most countries.[2,3] The most important reasons for poor prognosis are largely due to late diagnosis, a high postoperative recurrence rate, and metastasis.[4,5] Thus, a great challenge lies ahead in understanding the molecular mechanism of GC in identifying novel prognostic molecular biomarkers that can facilitate the development of appropriate therapeutic strategies earlier in GC.

Integrative genomic studies have shown that only 2% of DNA sequences can encode proteins, with more than 90% of these transcripts being actively transcribed; most of these transcripts are referred to as non-coding RNAs (ncRNAs).[6,7] Based on size, ncRNAs are divided into two groups, long non-coding RNAs (lncRNAs) over 200 nucleotides and small ncRNAs such as microRNAs (miRNAs).[8] Epigenetic modifiers, including lncRNAs and miRNAs, act to impact on human malignancies.[9–11] Currently, increasing studies show that lncRNAs usually interact with RNA-binding protein (RBP) to participate in a variety of biological processes, such as chromatin remodeling, transcriptional regulation, and RNA degradation.[12,13] Identification of lncRNA-dependent mechanisms of carcinogenesis is essential for understanding additional complexities of various tumors. Importantly, combined targeting of lncRNA-modulated key axes may provide a prospective rationale for cancer therapy.[11,14]

lncRNA TSPEAR-AS2 was previously reported to be involved in the regulation of hypoxia-induced pulmonary artery hypertension *in vitro*.[15] In this study, TSPEAR-AS2 is defined as a GC-associated lncRNA that we identified by analyzing The Cancer Genome Atlas

Received 3 August 2020; accepted 18 October 2020;
https://doi.org/10.1016/j.omtn.2020.10.022.

Correspondence: Ke-Ming Wang, Department of Oncology, The Second Clinical Medical College of Nanjing Medical University, Nanjing, Jiangsu, China.
E-mail: kemingwang@njmu.edu.cn
Correspondence: Xian-Zi Wen, Key Laboratory of Carcinogenesis and Translational Research (Ministry of Education), Division of Gastrointestinal Cancer Translational Research Laboratory, Peking University Cancer Hospital and Institute, Beijing, China.
E-mail: wenxz@bjmu.edu.cn
Correspondence: Jia-Fu Ji, Key Laboratory of Carcinogenesis and Translational Research (Ministry of Education), Division of Gastrointestinal Cancer Translational Research Laboratory, Peking University Cancer Hospital and Institute, Beijing, China.
E-mail: jijiafu@hsc.pku.edu.cn

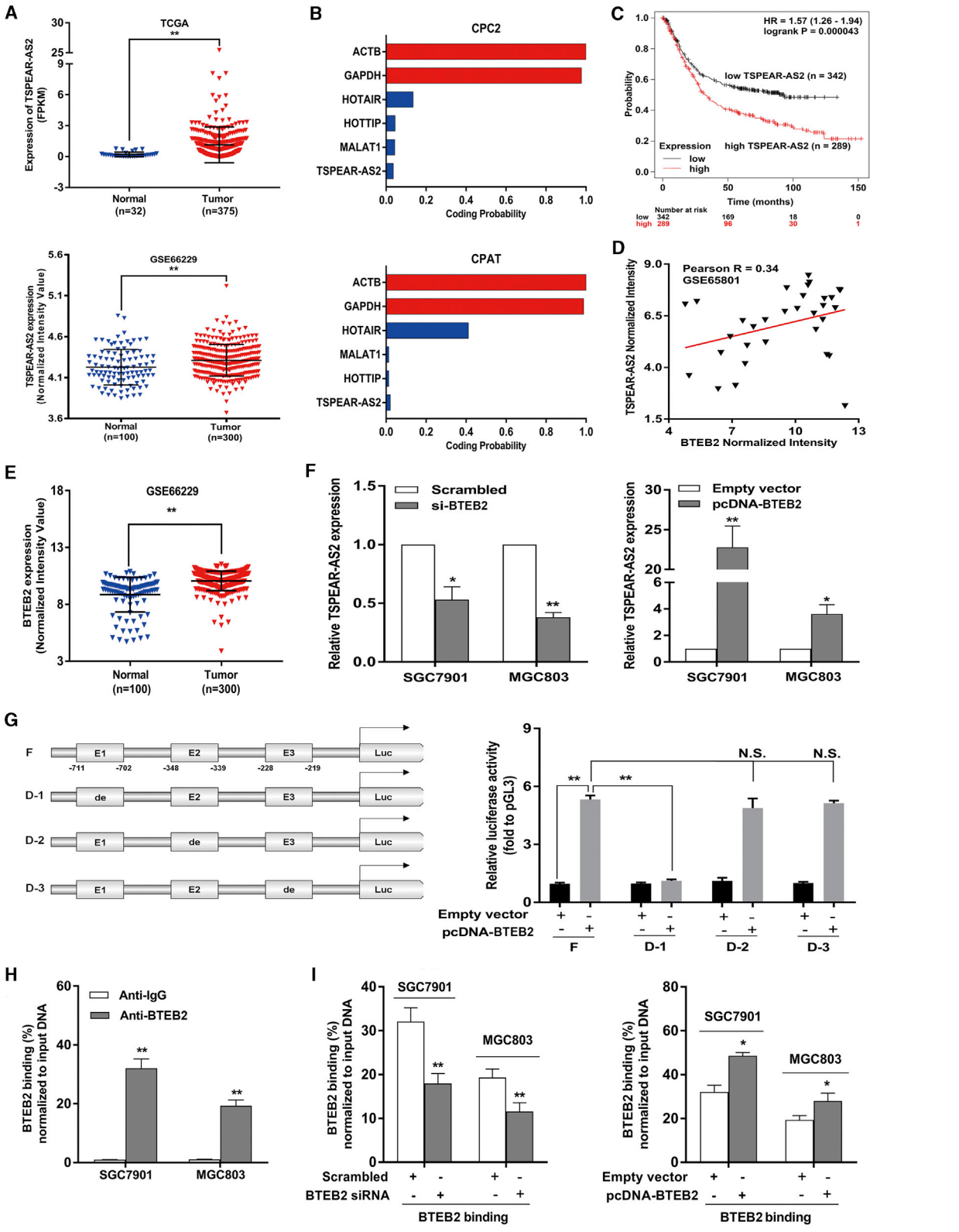

(legend on next page)

(TCGA) and Gene Expression Omnibus (GEO) datasets. Coding potential assessment tool (CPAT)[16] and coding potential calculator (CPC) analyses[17] predicted the low coding potential of lncRNA TSPEAR-AS2 (Figure 1B). It was shown that high TSPEAR-AS2 level closely associated with the overall survival (OS) of patients with GC, suggesting the predictive value of TSPEAR-AS2 in the prognosis of GC patients. Then, we demonstrated a mechanism by which overexpression of TSPEAR-AS2 in GC cells was activated by basic transcription element binding protein 2 (BTEB2). This mechanistic model of BTEB2/TSPEAR-AS2 was first elucidated in this research. *In vitro* and *in vivo* assays found that silencing of TSPEAR-AS2 markedly inhibited cell growth, migration, and invasion. By contrast, ectopic expression of TSPEAR-AS2 played an oncogenic role in GC progression. Based on the analysis of high-throughput RNA sequencing (RNA-seq), we identified the contribution of TSPEAR-AS2 and its key target gene gap junction protein alpha 1 (GJA1) in GC progression. Specifically, TSPEAR-AS2 epigenetically inhibited GJA1 expression through the interaction with polycomb repressive complex 2. Moreover, argonaute 2 (Ago2) was recruited by TSPEAR-AS2, which was defined to sponge miR-1207-5p, thereby contributing to the repression of claudin 4 (CLDN4) translation. In conclusion, our study aimed to characterize novel lncRNAs closely correlated with GC. The axis of enhancer of zeste 2 (EZH2)/GJA1 and miR-1207-5p/CLDN4 mediated by BTEB2-activated-TSPEAR-AS2 may provide new clues facilitating the identification of therapeutic targets as well as effective biomarkers for patients with GC.

RESULTS

lncRNA TSPEAR-AS2 Was Upregulated in GC and Tightly Associated with Survival Rates of Patients with GC

As an effort to identify lncRNAs closely correlated with GC, the publicly available data were downloaded from TCGA and GEO datasets. It was revealed that lncRNA TSPEAR-AS2 exhibited obvious upregulation in GC tissues (n = 375), as compared with normal tissues (n = 32) (Figure 1A). Moreover, the analysis of GSE66229 datasets demonstrated that TSPEAR-AS2 was obviously increased in GC tissues (n = 300) compared with normal tissues (n = 100) (Figure 1A). Additionally, TSPEAR-AS2 was markedly upregulated in GC cells compared with GES-1 cell line (Figure S1A). SGC7901 and MGC803 cells were selected for further research owing to their remarkable elevation of TSPEAR-AS2. Next, CPAT and CPC analyses were performed to reveal the low coding potential of lncRNA TSPEAR-AS2 (Figure 1B). To explore the correlation between TSPEAR-AS2 level and OS of patients, we also analyzed the publicly available data from 631 GC patients using Kaplan-Meier Plotter (http://kmplot.com/analysis/). As shown in Figure 1C, higher TSPEAR-AS2 expression closely associated with worse OS, highlighting the prognostic value of TSPEAR-AS2 in GC (Figure 1C).

TSPEAR-AS2 Was Transcriptionally Activated by Transcription Factor BTEB2 in GC

Currently, transcription factors (TFs) have been found to be capable of driving the expression of lncRNAs with tumor-promoting functions.[18,19] Therefore, we made assumptions that certain transcription factors were responsible for ectopic expression of TSPEAR-AS2. BTEB2, a zinc-finger transcription factor, has been identified to modulate activities correlated with various functions such as cell growth, proliferation, differentiation, and tumorigenesis.[20–22] It was shown that BTEB2 was significantly enriched in GC tissue samples (Figure 1E). Further analysis discovered the positive correlation between TSPEAR-AS2 and BTEB2 in GC tissue samples (Figure 1D). Then, we investigated the transcriptional regulation of TSPEAR-AS2 using JASPAR (http://jaspardev.genereg.net/) databases and found that BTEB2 can possibly bind to the promoter region of the TSPEAR-AS2 gene. The predicted binding regions are represented as E1, E2, and E3, shown in Figure 1G. In this regard, we deduced that BTEB2 might activate the transcription of TSPEAR-AS2. Therefore, the protein level of BTEB2 was first examined in GC cells with BTEB2 knockdown or overexpression. Compared with the control group, the protein level of BTEB2 was dramatically increased in GC cells with transfection of pcDNA-BTEB2 (Figure S1B). By contrast, small interfering RNAs (siRNAs) against BTEB2 obviously decreased the protein level of BTEB2 in GC cells (Figure S1B). Then, qRT-PCR assays were used to test the alteration of TSPEAR-AS2 in BTEB2-depleted or BTEB2-overexpressed GC cells. As expected, BTEB2 knockdown obviously decreased TSPEAR-AS2 expression, and BTEB2 overexpression markedly increased TSPEAR-AS2 expression, identifying BTEB2 as potential upstream regulator of TSPEAR-AS2 (Figure 1F).

To assess the transcription activation of BTEB2 on the promoter of TSPEAR-AS2, we cloned the promoter region of TSPEAR-AS2 into a luciferase reporter plasmid and made deletions at the promoter of TSPEAR-AS2 (Figure 1G). Then, cotransfection was performed in HEK293T cells with pcDNA-BTEB2/empty vector and luciferase reporter vectors TSPEAR-AS2 promoter full length (F), TSPEAR-AS2

Figure 1. High TSPEAR-AS2 Level Closely Associated with Poor Outcome of Patients with GC and the Transcription Factor BTEB2 Critically Activated the Transcription of TSPEAR-AS2

(A) Relative expression of TSPEAR-AS2 in GC tissues and normal tissues was measured in the data provided from GEO (GEO: GSE66229) and TCGA. (B) Evaluating the protein coding capacity of TSPEAR-AS2 through the Coding Potential Calculator 2 (CPC2) and Coding Potential Assessment Tool (CPAT). (C) The analysis of the correlation between TSPEAR-AS2 level and overall survival of GC patients (n = 631) using Kaplan-Meier Plotter. (D) The relationship between BTEB2 and TSPEAR-AS2 in GC tissue specimens was analyzed based on GSE65801 database. (E) BTEB2 levels in GC tissues and normal tissues were detected by analyzing data from GEO (GEO: GSE66229) database. (F) The effects of BTEB2 alteration on regulating the expression level of TSPEAR-AS2 in GC cells. (G) Dual-luciferase reporter assay was performed by co-transfecting the full TSPEAR-AS2 promoter fragment (pGL3-TSPEAR-AS2-F) or deleted TSPEAR-AS2 promoter fragment (pGL3-TSPEAR-AS2-D1, pGL3-TSPEAR-AS2-D2, pGL3-TSPEAR-AS2-D3) with pcDNA-BTEB2 or empty vector in HEK293T cells. (The predicted binding regions by JASPAR are represented as E1, E2, and E3.) (H) ChIP-qPCR assay showed direct binding of BTEB2 to endogenous TSPEAR-AS2 promoter regions in GC cells. (I) ChIP-qPCR assay showed BTEB2 enrichment on TSPEAR-AS2 promoter in GC cells transfected with BTEB2 siRNA or overexpression vector. *$p < 0.05$, **$p < 0.01$.

promoter deletion 1# (D-1), TSPEAR-AS2 promoter deletion 2# (D-2), or TSPEAR-AS2 promoter deletion 3# (D-3) (Figure 1G). Dual-luciferase reporter analysis showed that D-1 caused a significant downregulation in promoter activity compared with F, D-2, and D-3 (Figure 1G). These findings elucidated the binding of BTEB2 to this region and its efficacy of luciferase activation. Meanwhile, chromatin immunoprecipitation (ChIP) experiments were implemented. Our data demonstrated that BTEB2 directly bound to their binding sites on TSPEAR-AS2 promoter region in GC cells (Figure 1H). Furthermore, downregulation or overexpression of BTEB2 decreased or increased BTEB2 enrichment within the TSPEAR-AS2 promoter, respectively (Figure 1I). Taken together, our data demonstrated that increased TSPEAR-AS2 expression could be transcriptionally activated by the key transcription factor BTEB2 in GC.

TSPEAR-AS2 Boosted the Oncogenic Activities of GC Cells *In Vitro* and *In Vivo*

To illuminate the function of TSPEAR-AS2 in GC progression, we performed loss- and gain-of function assays to effectively alter TSPEAR-AS2 expression in GC cells (Figures 2A and 2B). Knockdown of TSPEAR-AS2 obviously inhibited GC cell proliferation and impaired colony-formation ability (Figures 2C and 2E), while TSPEAR-AS2 overexpression displayed the reverse effects (Figures 2D and 2F). Moreover, Ethynyldeoxyuridineanaly (EdU) assays verified that TSPEAR-AS2 knockdown obviously decreased the proliferative capacities of GC cells (Figure 2G). Flow cytometry assays demonstrated that inhibition of TSPEAR-AS2 significantly increased the proportion of apoptosis in GC cells (Figure 2H). Our data verified that the inhibition of cell proliferation induced by TSPEAR-AS2 knockdown could be partly attributed to activated apoptosis in GC cells. In addition, TSPEAR-AS2 repression markedly weakened the migratory and invasive capacities of GC cells (Figures 2I and S2A), and overexpression of TSPEAR-AS2 elicited the opposite impacts (Figures 4K and S2B).

To determine TSPEAR-AS2 impact on tumorigenic capacities *in vivo*, a xenograft tumor model was constructed. TSPEAR-AS2-stable-knockdown MGC803 cells or control cells were subcutaneously injected into male nude mice. We found that the tumors derived from the control group were markedly larger than tumors obtained from the TSPEAR-AS2-stable-knockdown group (Figure 2J). Additionally, the volume and weight of the tumors formed from TSPEAR-AS2-stable-knockdown group were significantly decreased compared with those derived from the control group, indicating the promotion effects of TSPEAR-AS2 on the tumorigenic abilities of GC cells (Figures 2K and 2L). As shown in Figures 2M and 2N, tumors derived from the control group revealed stronger staining of Ki-67 compared with tumors obtained from the TSPEAR-AS2-stable-knockdown group (Figures 2M and 2N).

Silencing of GJA1 Was Regulated by Interaction of TSPEAR-AS2 and Polycomb Repressive Complex 2

To uncover the underlying mechanism about how lncRNA TSPEAR-AS2 contribute to the malignant phenotype of GC, we evaluated the gene expression profiles of a control group and TSPEAR-AS2 knockdown group via RNA-seq (Figures 3A and 3B). Gene Ontology (GO) analysis of RNA-seq assays of TSPEAR-AS2 knockdown demonstrated that the alteration in gene set was closely associated with cell migration, cell proliferation, apoptotic process, and cell growth (Figure 3D). As shown in Figures 3E and 3F, Gene Set Enrichment Analysis (GSEA) was applied to further explore the pathways involved in GC pathogenesis. Enrichment plots of GSEA highlighted that the gene signatures of negative regulation of growth and positive regulative extrinsic apoptotic signaling pathway were much more involved in TSPEAR-AS2-depleted cells compared with the control group (Figures 3E and 3F). Then, qRT-PCR assays were used to identify key regulators mediated by TSPEAR-AS2 knockdown and thus further the understanding of TSPEAR-AS2-mediated GC progression. Among these aberrantly altered key genes, GJA1 displayed the highest level in TSPEAR-AS2-depleted SGC7901 cells relative to the control group (Figure 3C). Current evidence has demonstrated that GJA1 exhibits close association with cancer development, distant metastasis, and survival condition.[23,24] Moreover, GJA1 was dramatically upregulated in TSPEAR-AS2-depleted GC cells, as demonstrated by qRT-PCR and western blot experiments (Figures 3G and 3H).

To further clarify TSPEAR-AS2-involved regulatory mechanisms in GC progression, we performed subcellular fractionation and RNA-fluorescence *in situ* hybridization (FISH) assays in GC cells. Our findings elucidated that TSPEAR-AS2 was more prevalent in the nucleus than in the cytoplasm in SGC7901 and MGC803 cells (Figures 4A and 4B). These findings may support the potential transcriptional regulation of TSPEAR-AS2 in GC progression. Currently, researchers demonstrated that lncRNAs could modulate epigenetic modification or gene silencing through binding with RBPs.[25,26] To further determine the regulatory mechanism of TSPEAR-AS2-induced GJA1 silencing, bioinformatics analysis was first conducted to predict interaction possibilities of RBPs and TSPEAR-AS2. The analysis data indicated that TSPEAR-AS2 was predicted to potentially bind with EZH2, SUZ12, EED, STAU1, and Ago2, with the score of RF or SVM greater than 0.5 (Figure 4C). To verify this prediction, radioimmunoprecipitation (RIP) assays testified the binding of TSPEAR-AS2 with EZH2, SUZ12, and AGO2 in GC cells (Figure 4D).

Methyltransferase EZH2, a critical member of PRC2, enhances methylation of H3K27, leading to silencing of tumor suppressors.[27,28] The amplification of EZH2 was observed in various types of cancers.[29–31] Previous research also highlighted the oncogenic role of EZH2 in GC, indicating its emerging role in this active field.[32] In this study, the level of EZH2 was effectively impaired in GC cells with siRNAs against EZH2 (Figure S3A). Intriguingly, knockdown of EZH2 can dramatically upregulate GJA1 level in GC (Figure S3B). Together, GJA1 may be coregulated by TSPEAR-AS2 and EZH2 in GC.

To elucidate whether TSPEAR-AS2 was involved in regulating gene transcription by recruiting PRC2, we performed ChIP assays in

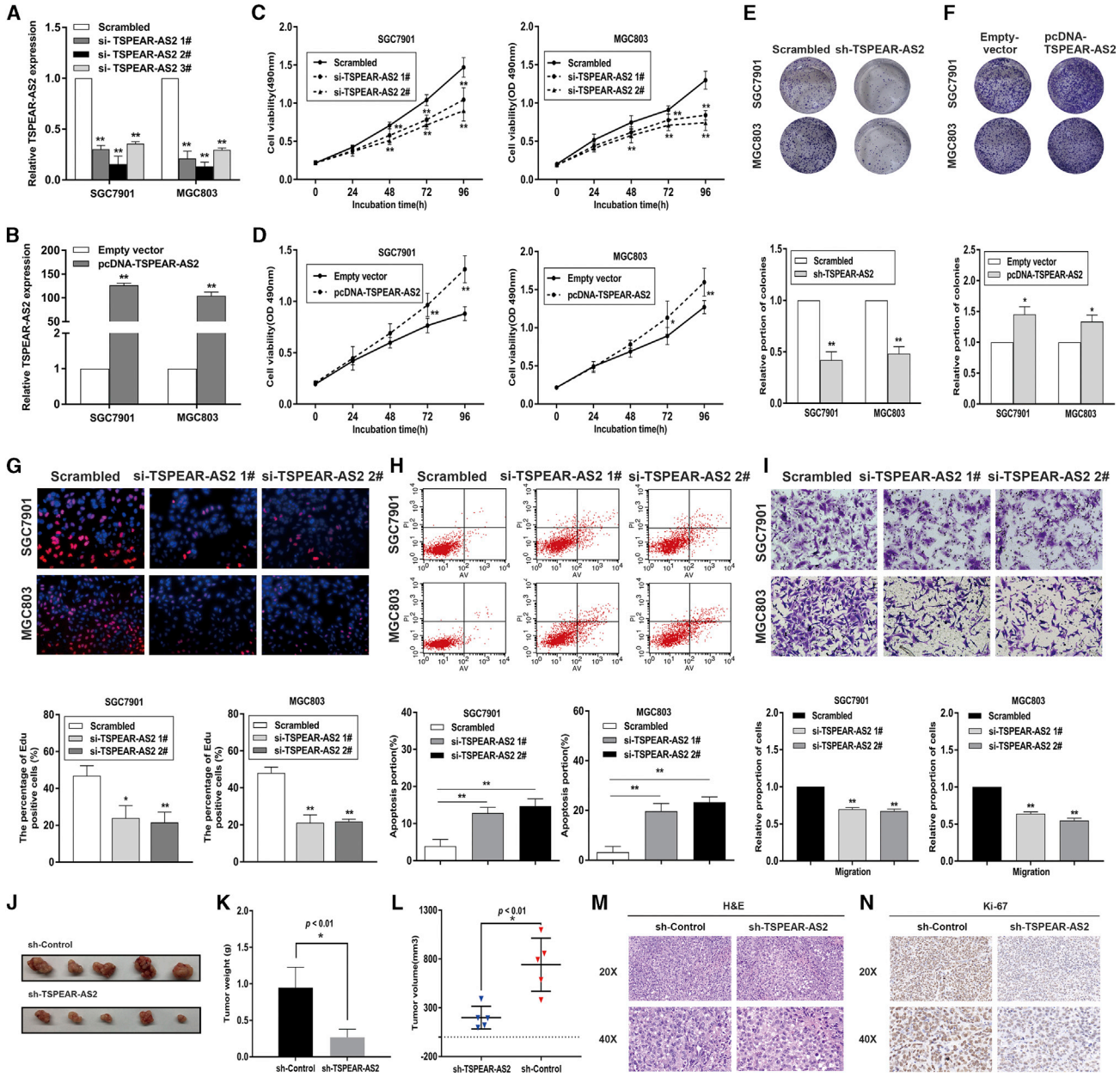

Figure 2. The Biological Role of TSPEAR-AS2 in GC Progression

(A) TSPEAR-AS2 knockdown efficiency was analyzed by qRT-PCR in GC cells. **(B)** TSPEAR-AS2 overexpression efficiency was analyzed by qRT-PCR in GC cells. **(C)** Cell viability examinations of GC cells with TSPEAR-AS2 knockdown. **(D)** Cell viability examinations of GC cells with TSPEAR-AS2 overexpression. **(E)** Colony-forming assays were conducted to determine the proliferation of GC cells with TSPEAR-AS2 knockdown. **(F)** Colony-forming assays were conducted to determine the proliferation of GC cells with TSPEAR-AS2 overexpression. **(G)** Cell proliferation of GC cells was evaluated 48h after transfection with TSPEAR-AS2 siRNAs or Scrambled using EdU assays. **(H)** The apoptosis of GC cells transfected with TSPEAR-AS2 siRNAs or Scrambled was analyzed by flow cytometry assays. **(I)** Transwell assays were performed in GC cells transfected with TSPEAR-AS2 siRNAs or Scrambled. **(J)** The dissected tumors bearing from MGC803 cells transfection of sh-Control or shRNA groups. **(K)** The weight of tumors obtained from sh-TSPEAR-AS2 group or control group. **(L)** The volume of tumors obtained from sh-TSPEAR-AS2 group or control group. **(M)** H&E staining of the tumors isolated from mice. 20×images and 40×images were shown. **(N)** Ki-67 staining of the tumors isolated from mice. 20×images and 40×images were shown. *$p < 0.05$, **$p < 0.01$.

SGC7901 and MGC803 cells. It was demonstrated that TSPEAR-AS2 knockdown significantly reduced the binding of EZH2 and H3K27me3 across the GJA1 promoter region (Figure 4G). Together, our data revealed that TSPEAR-AS2 participate in the tumorigenesis of GC through the transcriptional regulation of GJA1 via binding to PRC2 in GC cells.

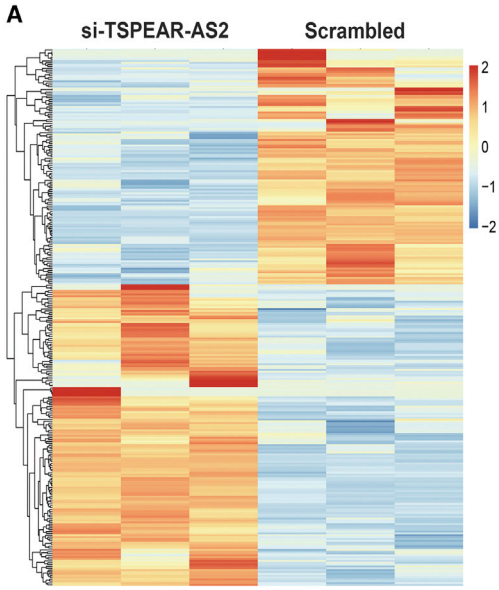

C

log2FC	GJA1	HDAC9	ROS1	ANKRD1	XAF1
RNA-seq	2.73	2.05	2.04	1.96	1.77
qRT-PCR	2.95	2.05	1.65	1.08	2.07

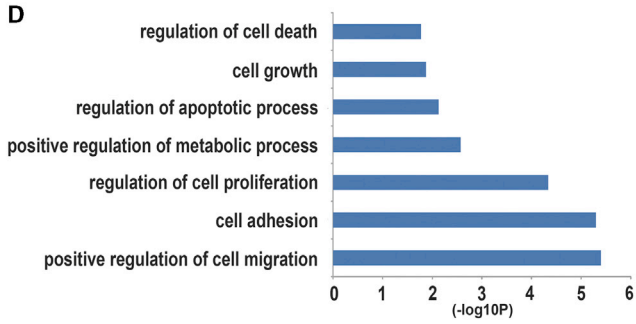

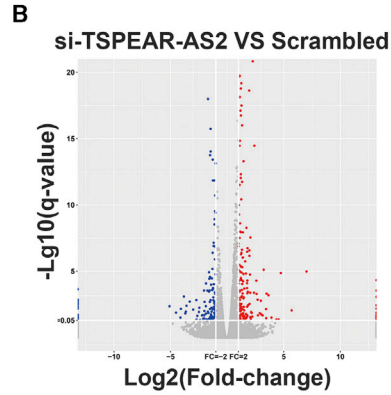

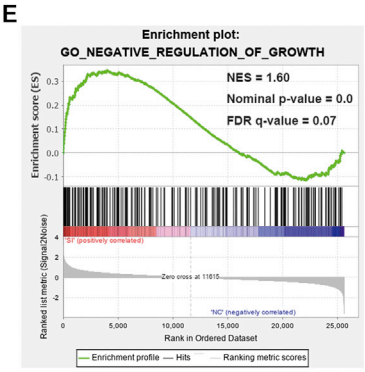

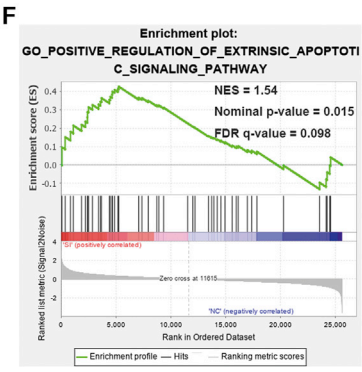

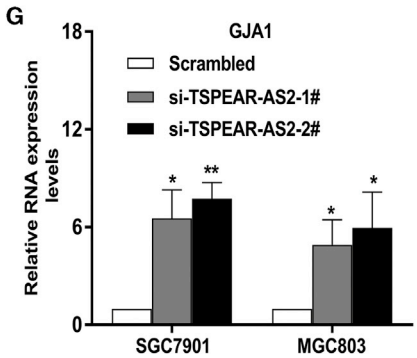

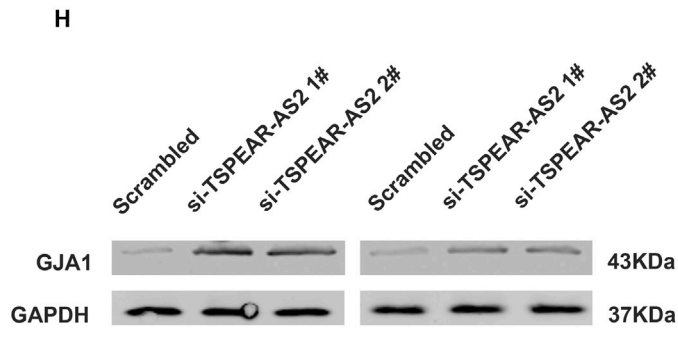

Figure 3. GJA1 Acted as a Key Downstream Target of TSPEAR-AS2 in GC Progression

(A) Heatmap of altered genes in GC cells transfected with TSPEAR-AS2 siRNA or Scrambled. (B) Hierarchical clustering gene transcription altered in GC cells after knockdown of TSPEAR-AS2. (C) The qRT-PCR assays were conducted to validate the level of key genes in GC cells with TSPEAR-AS2 knockdown. (D) Gene Ontology analysis for all genes with altered expressions after knockdown of TSPEAR-AS2. (E) GSEA explored the gene sets enriched by genes in response to TSPEAR-AS2 knockdown (Negative regulation of growth). **(F)** GSEA explored the gene sets enriched by genes in response to TSPEAR-AS2 knockdown (Positive regulation of extrinsic apoptotic signaling pathway). (G) The expression of GJA1 was determined in GC cells treated with TSPEAR-AS2 siRNA or scrambled using qRT-PCR assays. **(**H) The expression of GJA1 was determined in GC cells treated with TSPEAR-AS2 siRNA or scrambled using western blot assays. *$p < 0.05$, **$p < 0.01$.

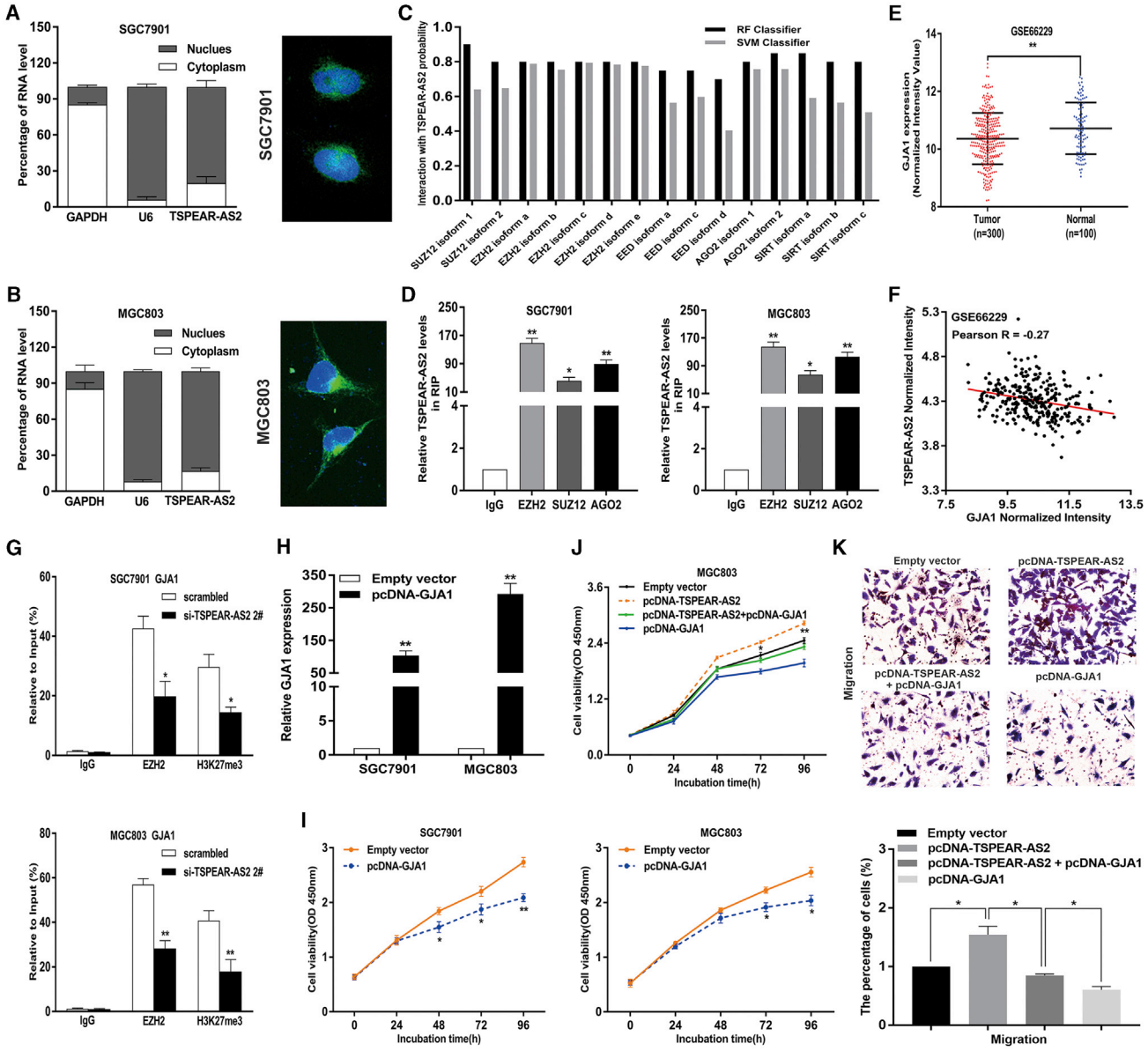

Figure 4. lncRNA TSPEAR-AS2 Silenced GJA1 Transcription through Binding to EZH2 in GC

(A) The subcellular localization analysis of the location of TSPEAR-AS2 in the cytoplasm and nuclear fractions in GC cells. (B) The FISH analysis of the location of TSPEAR-AS2 in the cytoplasm and nuclear fractions in GC cells. (C) Prediction of the interaction probability between TSPEAR-AS2 and RNA binding proteins by bioinformatics (http://pridb.gdcb.iastate.edu/RPISeq/). (D) The interaction of TSPEAR-AS2 with EZH2, SUZ12, and AGO2 was verified by RIP assay in GC cells. (E) The expression of GJA1 in GC tissues compared with normal tissues in GSE66229 datasets. (F) The correlation between the level of TSPEAR-AS2 and GJA1 in GC tissues was detected using data from GSE66229 datasets. (G) ChIP-qPCR assay of EZH2 and H3K27me3 occupancy in the GJA1 promoter in GC cells transfected with TSPEAR-AS2 siRNA or Scrambled. (H) The expression level of GJA1 is detected in GC cells transfected with pcDNA-GJA1 through qRT-PCR. (I) The effects of GJA1 overexpression on GC cell viability were detected using CCK8 assays. (J) Overexpression of GJA1 can partly reverse the promotion effects of GC cell proliferation mediated by TSPEAR-AS2 overexpression. (K) Overexpression of GJA1 can partly reverse the promotion effects of GC cell migration mediated by TSPEAR-AS2 overexpression. *p < 0.05, **p < 0.01.

Oncogenic Function of TSPEAR-AS2 by Repressing GJA1 Expression

Given the potential regulatory role of GJA1 in TSPEAR-AS2-involved GC progression, bioinformatics analysis was implicated to verify the expression pattern of TSPEAR-AS2 in specimens from patients with GC. It was shown that GJA1 was prominently downregulated in GC tissue samples (n = 300) compared with non-tumor samples (n = 100) (Figure 4E). Meanwhile, it is interesting to note the negative relationship between GJA1 level and TSPEAR-AS2 level in GC tumor specimens (n = 300) (Figure 4F).

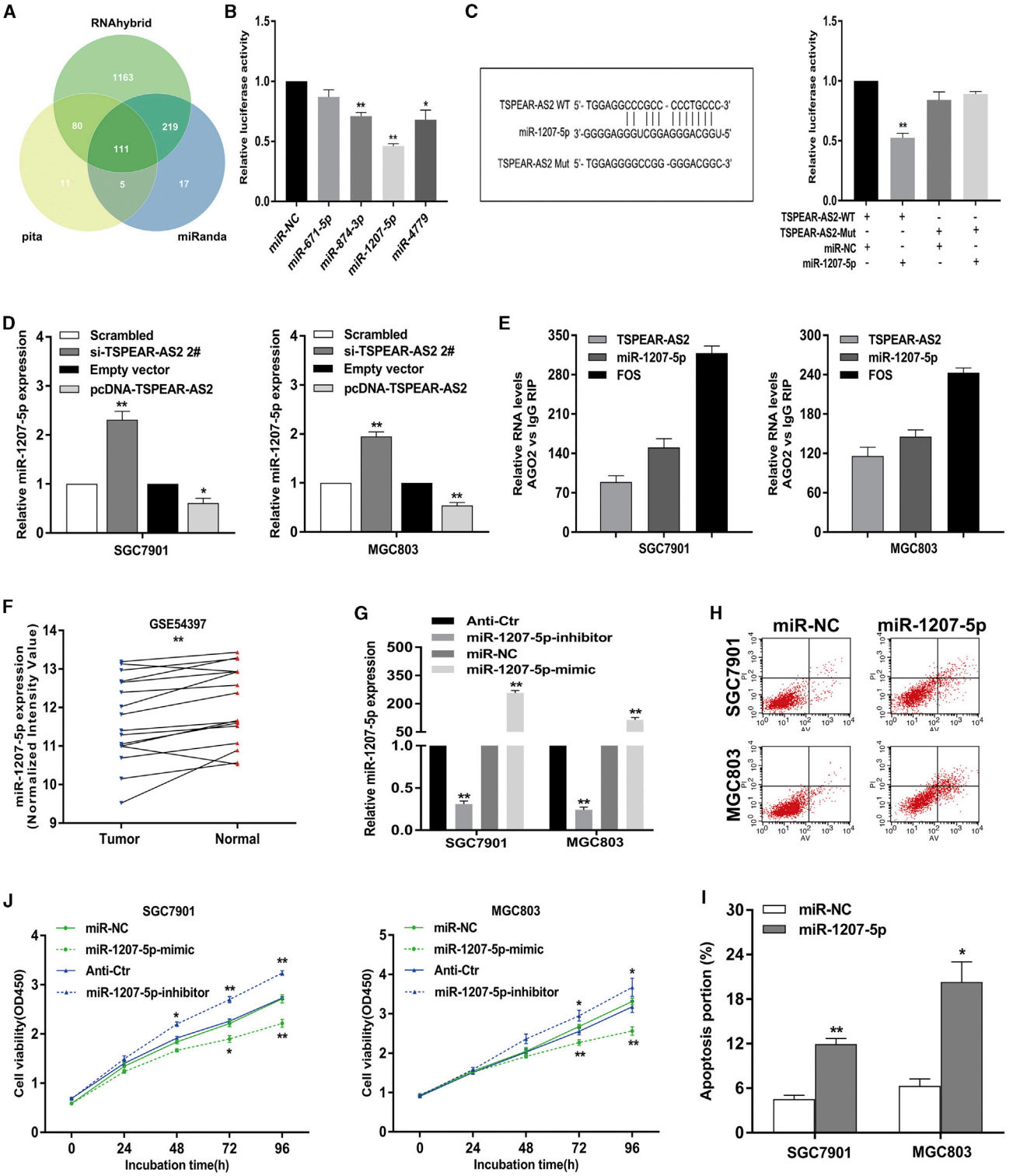

Figure 5. Regulation Relationship between lncRNA TSPEAR-AS2 and miR-1207-5p in GC

(A) Bioinformatics databases (miRanda, pita, and RNAhybrid) were analyzed to predict potential miRNAs binding with TSPEAR-AS2. (B) Luciferase activity of HEK293T cells cotransfected with 4 various miRNA-coding plasmids and the luciferase reporter plasmids (pmirGLO-TSPEAR-AS2-WT). Data are presented as the ratio of firefly luciferase to

(legend continued on next page)

In addition, the level of GJA1 was verified in GC cells treated with empty vector or pcDNA-GJA1. It can be observed that GC cells with pcDNA-GJA1 displayed remarkable upregulation compared with the control group (Figure 4H). Cell viability tests verified the inhibition impact of GJA1 overexpression on GC cell proliferation (Figure 4I).

To investigate the function of GJA1 in TSPEAR-AS2-induced promotion of GC proliferation, invasion, and migration, rescue assays were conducted in GC cells, which were cotransfected with pcDNA-TSPEAR-AS2 and pcDNA-GJA1. Of note, ectopic expression of TSPEAR-AS2 remarkably activated GC cell proliferation, migration, and invasion, and overexpression of GJA1 was capable of reversing the influence mediated by TSPEAR-AS2 (Figures 4J, 4K, and S2B). These data elucidated that the effects of TSPEAR-AS2 on GC progression may partially depend on the regulation of GJA1.

lncRNA TSPEAR-AS2 Elevated CLDN4 Expression through Competing for miR-1207-5p

Importantly, TSPEAR-AS2 may also play a post-transcriptional role in gene regulation. It is known that lncRNAs have been implicated in post-transcription regulation, such as sponging activity for miRNAs.[33,34] To investigate whether TSPEAR-AS2 played such a role, we used miRanda, pita, and RNAhybrid to make a prediction of possible miRNAs targeting sites on TSPEAR-AS2 (Figure 5A). According to the prediction result and current evidence, we filtered out a number of miRNAs, which have been shown to inhibit the malignant phenotype of tumor.[35–37] Therefore, the implementation of dual-luciferase reporter assays testfied the interacted correlation between TSPEAR-AS2 and these miRNAs. We observed that the luciferase activity of pmir-GLO-TSPEAR-AS2 that contained full-length TSPEAR-AS2 can be significantly repressed by the transfection of miR-874-3p, miR-1207-5p, and miR-4779 (Figure 5B). Moreover, miRNA-1207-5p showed the strongest inhibition effect (Figure 5B). Thus, miR-1207-5p was selected for further analysis.

Thereafter, site-targeted mutagenesis was constructed within the speculative miR-1207-5p-binding site in the lncRNA TSPEAR-AS2 sequence (Figure 5C). It was shown that pmir-GLO-TSPEAR-AS2-mut (TSPEAR-AS2-Mut) failed to respond to miR-1207-5p, clarifying that TSPEAR-AS2 acts to sponge miR-1207-5p (Figure 5C). In addition, knockdown of TSPEAR-AS2 gave rise to an elevated level of miR-1207-5p, whereas the boosted TSPEAR-AS2 level reflected contrary impact on miR-1207-5p level in GC cells (Figure 5D). However, overexpression of miR-1207-5p displayed no significant difference on TSPEAR-AS2 expression (Figure S3C). More importantly, RIP assays were performed in GC cells to verify whether TSPEAR-AS2 and miR-1207-5p were involved in the RNA-induced silencing complex (RISC). It was shown that both TSPEAR-AS2 and miR-1207-5p are drastically enriched in AGO2 immunoprecipitates compared with those in the immunoglobulin G (IgG) pellet in SGC7901 and MGC803 cells (Figure 5E). These results suggested that TSPEAR-AS2 physically existed in the AGO2-based miRNA-modulated repression complex and exhibited close association with miR-1207-5p, but miR-1207-5p did not induce TSPEAR-AS2 degradation.

Previous evidence has indicated that miR-1207-5p is of great significance in many fetal malignancies.[38,39] Nevertheless, the functional biology of miR-1207-5p was not comprehensively elucidated in GC. Furthermore, the mechanistic model of miR-1207-5p in TSPEAR-AS2-mediated GC progression remains unclear. Therefore, the profile of the miR-1207-5p level was verified in paired tissue specimens from patients with GC (GSE54397) (Figure 5F). The significant downregulation of miR-1207-5p can be observed in GC tissue samples relative to matched normal tissue samples (Figure 5F). Then, significant overexpression or knockdown of miR-1207-5p level was made in GC cells using mimic or inhibitor against miR-1207-5p (Figure 5G). We gave the first evidence that the ectopic level of miR-1207-5p dramatically improve the apoptotic proportion of GC cells (Figures 5H and 5I). Consistently, knockdown of miR-1207-5p could obviously activate GC cell proliferation (Figure 5J). By contrast, elevation of miR-1207-5p impacted contrary effects on GC cell proliferation (Figure 5J). These findings highlight the critical role of miR-1207-5p in TSPEAR-AS2-correlated GC progression

To detail the TSPEAR-AS2-involved mechanism of post-transcriptional regulation, data mining was processed in RNA-seq analysis of a control group and the TSPEAR-AS2-knockdown group. We observed that a number of key genes displayed obvious downregulation in abundance of log2FC (fold change) ≤ -1 (Figure 3B). Then, a series of verification experiments were applied to test the alteration after TSPEAR-AS2 knockdown. It was found that a number of key genes were dramatically decreased in TSPEAR-AS2-depleted GC cells, including CLDN4, solute carrier family 25 member 10 (SLC25A10), phospholipase C eta 2 (PLCH2), and sushi domain containing 2 (SUSD2), in both SGC7901 and MGC803 cells. Among these potential genes, TSPEAR-AS2 knockdown displayed the strongest inhibition effects on CLDN4 level (Figure 6A). It is known that the alteration of CLDN4 is tightly linked with the malignant progression of various malignancies and therapeutic resistance.[40–42] Here, we found the obvious downregulation of CLDN4 in TSPEAR-AS2-depleted GC cells and significant upregulation of CLDN4 in TSPEAR-AS2-overexpressed GC cells, identifying that CLDN4 may

Renilla luciferase activity. (C) Luciferase activity in HEK293T cells cotransfected with miR-1207-5p or negative control and pmirGLO-TSPEAR-AS2-WT or pmirGLO-TSPEAR-AS2-Mut. (D) The level of miR-1207-5p was examined in GC cells with TSPEAR-AS2 knockdown or overexpression through qRT-PCR assays. (E) RNA levels in immunoprecipitates were presented as fold change in Ago2 relative to IgG immunoprecipitates. (F) Relative expression of miR-1207-5p in GC tissues and paired normal tissues was analyzed in the GSE54397 database. (G) The level of miR-1207-5p was detected in GC cells transfected with mimic or inhibitor against miR-1207-5p using qRT-PCR assays. (H and I) The effects of miR-1207-5p on GC cell apoptosis were analyzed by flow cytometry assays. (J) The effects of miR-1207-5p knockdown or overexpression on GC cell viability. $^{*}p < 0.05$, $^{**}p < 0.01$.

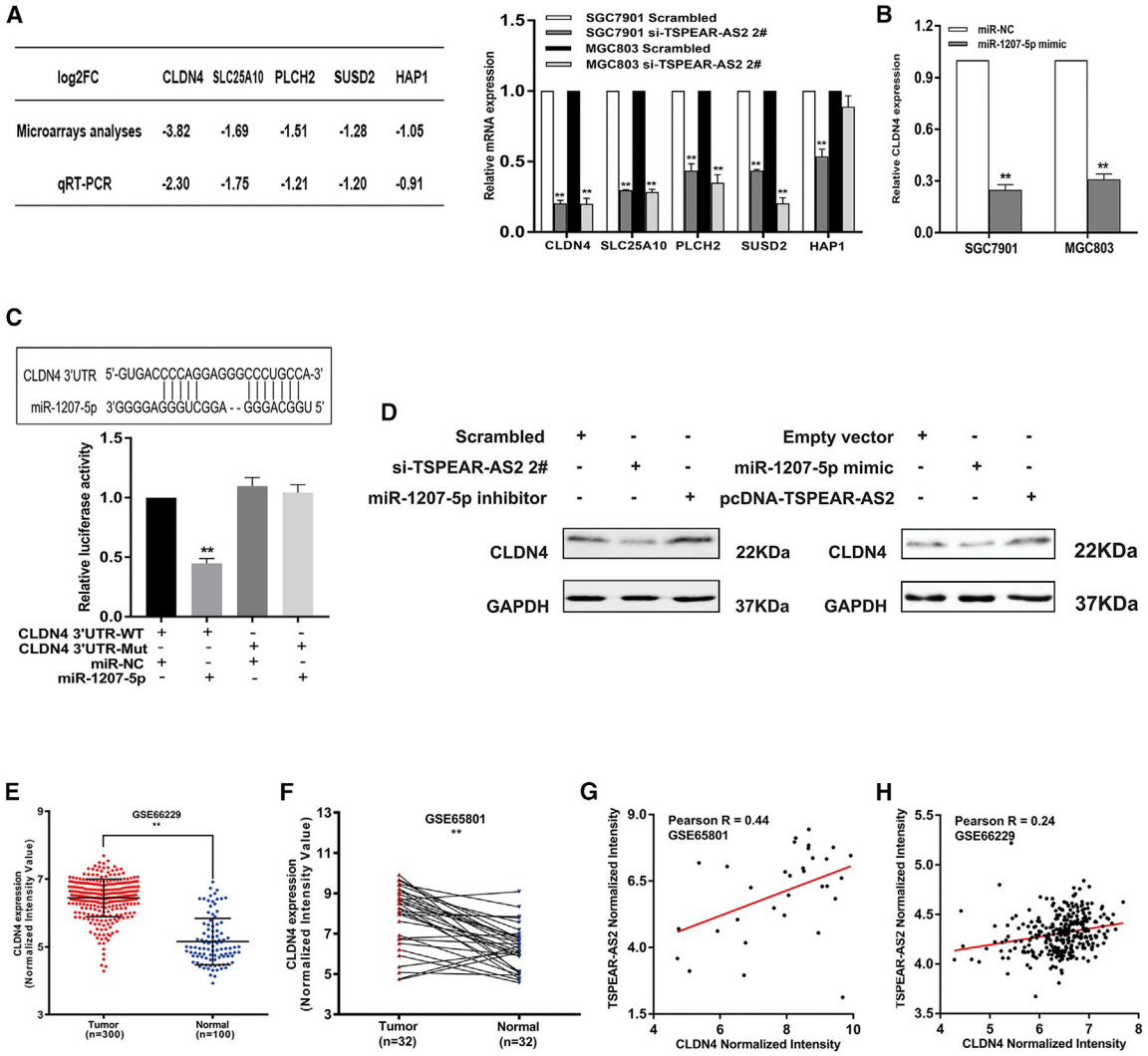

Figure 6. lncRNA TSPEAR-AS2 Modulates CLDN4 Expression by Competing for miR-1207-5p in GC

(A) The qRT-PCR assays were conducted to validate the alteration of key genes in GC cells with TSPEAR-AS2 knockdown. (B) The effects of miR-1207-5p overexpression on CLDN4 expression in GC cells. (C) Luciferase activity in HEK293T cells cotransfected with miR-1207-5p or negative control and pmirGLO-CLDN4 3′UTR-WT or pmirGLO-CLDN4 3′UTR-Mut. (D) Western blot assay was used to detect CLDN4 protein level in GC cells upon miR-1207-5p mimic or pcDNA-TSPEAR-AS2 treatment (right), and in the absence of TSPEAR-AS2 expression or miR-1207-5p inhibitor (left). (E) The level of CLDN4 in gastric cancer tissues and normal tissues was measured in the data provided from GEO (GSE66229) datasets. (F) The level of CLDN4 in gastric cancer tissues and normal tissues was measured in the data provided from GEO (GSE65801) datasets. (G) The relationship between CLDN4 and TSPEAR-AS2 in GC tissues was determined based on the data from GSE65801 datasets. (H) The relationship between CLDN4 and TSPEAR-AS2 in GC tissues was determined based on the data from GSE66229 datasets.

be a key downstream effector of TSPEAR-AS2 in GC progression (Figure 6D).

Subsequently, we assumed that TSPEAR-AS2, miR-1207-5p, and CLDN4 were involved in a competing endogenous RNA (ceRNA) regulatory network. To verify our hypothesis, we first performed miR-1207-5p overexpression assays in GC cells and found that the elevation of miR-1207-5p resulted in the obvious decrease of CLDN4 at the mRNA level (Figure 6B). Moreover, we further revealed that the depletion or increase of miR-1207-5p can significantly upregulate or downregulate CLDN4 expression in GC cells (Figure 6D). Interestingly, the prediction analysis from miRanda database showed that miR-1207-5p can possibly bind to CLDN4 (Figure 6C). As shown in Figure 6C, a luciferase activity assay further demonstrated that miR-1207-5p elevation induced the effective suppression of luciferase activity of CLDN4-3′ UTR-wild-type (WT) but not CLDN4-3′ UTR-Mut (Figure 6C). The analysis of GSE66229 database highlighted the abundance of CLDN4 in GC tissue specimens (n = 300) compared with normal specimens (n = 100) (Figure 6E). We also detected the CLDN4 level in paired

specimens from patients with GC and indicated CLDN4 upregulation in GC (Figure 6F). Interestingly, the positive correlation can be observed between TSPEAR-AS2 and CLDN4 in GC tumor samples, highlighting the tight regulatory correlation between TSPEAR-AS2 and CLDN4 in GC progression based on data from GEO datasets (GEO: GSE65801 and GSE66229) (Figures 6G and 6H). Taken together, our findings elucidated that lncRNA TSPEAR-AS2 worked as a ceRNA for miR-1207-5p, consequently leading to a boosted level of CLDN4 in GC progression.

DISCUSSION

Mounting evidence has reported that lncRNAs are effective biological regulators rather than "transcriptional noise."[11,43–45] Despite that lncRNAs have been considered to play important roles during cancer progression, a variety of mechanisms need to be developed and clarified in various types of cancers, especially GC. To detect lncRNAs potentially involved in GC progression, we first explored the publicly available profiling data of GC from TCGA and GEO datasets. A novel lncRNA, TSPEAR-AS2, was screened out as a candidate gene associated with GC progression. The ectopic expression of TSPEAR-AS2 exhibited close correlation with the survival condition of patients with GC. Through gain- and loss-of function assays, TSPEAR-AS2 could induce GC cell apoptosis and promote GC proliferation, migration, and invasion. Together, TSPEAR-AS2 may exhibit an oncogenic role in GC progression. To the best of our knowledge, this is the first study to systematically evaluate the role of TSPEAR-AS2 in GC initiation and development.

Current studies indicate that many transcription factors have been revealed to be highly expressed in various malignancies, contributing to the activities of transcriptional activation of lncRNAs.[46,47] In this study, a high level of transcription factor BTEB2 was observed in GC specimens and potentially correlated with TSPEAR-AS2 abundance, contributing to TSPEAR-AS2 overexpression in GC. Both FISH and subcellular fractionation assays demonstrated that TSPEAR-AS2 was more prevalent in the nucleus of GC cells, suggesting that TSPEAR-AS2 may mediate GC progression at the transcriptional level. RNA-seq found that inhibition of TSPEAR-AS2 affected key regulators correlated with cancer, such as GJA1, HDAC9, ROS1, ANKRD1, and XAF1. The expression level of GJA1 exhibited significant upregulation in GC cells with knockdown of EZH2, which is a critical member of PRC2. Interestingly, GJA1 can be coregulated by TSPEAR-AS2/EZH2. Mechanistic assays showed that TSPEAR-AS2 may participate in the tumorigenesis of GC via transcription repression of key regulators through interaction with EZH2. Additionally, TSPEAR-AS2-induced GC proliferation, migration, and invasion can be significantly reversed by overexpression of GJA1 in GC.

Recently, a novel regulatory mechanism has been illuminated to exist between lncRNAs and miRNAs in many malignant diseases.[48–50] Both lncRNAs and miRNAs exert dynamic function in transcriptional and translational regulation.[51,52] lncRNAs can serve as ceRNAs to protect mRNAs through competing for their targeting miRNAs.[49–51] In the present study, bioinformatics databases (miRanda, pita, and RNAhybrid) were analyzed to predict miRNAs, which may potentially bind with TSPEAR-AS2. Among these miRNAs, miR-1207-5p showed the strongest repressive abilities of TSPEAR-AS2-mediated luciferase activity. Furthermore, RNA-seq assays and verified assays confirmed that CLDN4 is among the most downregulated gene in GC cells with TSPEAR-AS2 knockdown. Subsequently, a series of assays were designed to determine the novel ceRNA network formed by TSPEAR-AS2, miR-1207-5p, and CLDN4. TSPEAR-AS2 knockdown or overexpression could obviously boost or impair the level of miR-1207-5p, while miR-1207-5p elevation had no impact on TSPEAR-AS2 regulation. RIP assays revealed that both TSPEAR-AS2 and miR-1207-5p were involved in the same RISC. Dual-luciferase-reporter assays clarified the direct binding ability of the predicted miR-1207-5p binding site on TSPEAR-AS2 and further demonstrated that miR-1207-5p could directly target CLDN4 in GC. These data strongly indicated that TSPEAR-AS2 could serve as a ceRNA for miR-1207-5p to regulate CLDN4 expression at the post-transcriptional level in GC. Rescue assays further revealed that CLDN4 knockdown can, at least in part, reverse the promotion of GC progression caused by overexpressing TSPEAR-AS2.

In summary, this is the first report documenting the clinical value, biological role, and mechanism of TSPEAR-AS2 in GC. The BTEB2-activated TSPEAR-AS2 model was first elucidated in this study, leading to TSPEAR-AS2 transcription promotion in GC. Meanwhile, TSPEAR-AS2 could serve as a ceRNA for miRNAs or interact with PRC2 in GC. Our data highlight the key involvements of TSPEAR-AS2 in GC progression, implicating the axis of TSPEAR-AS2/EZH2/GJA1 and TSPEAR-AS2/miR-1207-5p/CLDN4 as novel targets for GC therapeutics. Importantly, the investigation of the expression and mechanistic model of TSPEAR-AS2 in other GC cells is urgently needed in future research. More explorations are also required to detect other upstream effectors or downstream effectors of TSPEAR-AS2 in GC progression.

MATERIALS AND METHODS

Cell Culture

Human gastric adenocarcinoma cancer cell lines and normal gastric epithelium cell line (GES-1) were maintained as previously reported.[53]

RNA Immunoprecipitation

We used EZMagna RIP Kit (Millipore, Billerica, MA, USA) to perform RIP assays in GC cell lines. The detailed information is summarized in the Supplemental Information. The details for antibodies, primers, and siRNA oligonucleotides are listed in Table S1.

Luciferase Assays

Luciferase assays were performed as previously described.[53]

Chromatin Immunoprecipitation Assays

EZ-ChIP Kit (Millipore, Billerica, MA, USA) was used to conduct ChIP assays in accordance with the manufacturer's instructions.

The details of ChIP procedures can be found in the Supplemental Information.

Statistical Analysis

SPSS version 25.0 software was used to assess statistical differences. The significance between groups was assessed using a paired, two-tailed Student's t test, Wilcoxon test, or χ^2 test. The curves of OS were obtained using the Kaplan-Meier method. $p < 0.05$ was indicative of significant difference.

SUPPLEMENTAL INFORMATION

Supplemental Information can be found online at https://doi.org/10.1016/j.omtn.2020.10.022.

ACKNOWLEDGMENTS

This study was funded by the Innovation Fund for Outstanding Doctoral Candidates of Peking University Health Science Center (grant number: 71013Y2029); the Cancer Hospital Foundation of Jiangsu (grant number: ZM201907); the National Natural Science Foundation of China (81772603); the Science Foundation of Peking University Cancer Hospital (2017-23, A001538); and the Peking University Clinical Scientists Program (BMU2019LCKXJ011), supported by the Fundamental Research Funds for the Central Universities.

AUTHOR CONTRIBUTIONS

Z.H.M., Y.S., K.M.W., X.Z.W., and J.F.J. designed the whole study. Z.H.M. drafted the manuscript and prepared the figures. Z.H.M., Y.S., X.Y.G., and Y.Y. performed *in vitro* assays and data analysis. Y.S. performed *in vivo* assays and bioinformatics analysis. K.M.W., X.Z.W., and J.F.J. provided full guidance. All authors have read and approved the final version.

DECLARATION OF INTEREST

The authors declare no competing interests.

REFERENCES

1. Arnold, M., Park, J.Y., Camargo, M.C., Lunet, N., Forman, D., and Soerjomataram, I. (2020). Is gastric cancer becoming a rare disease? A global assessment of predicted incidence trends to 2035. Gut *69*, 823–829.
2. Bray, F., Ferlay, J., Soerjomataram, I., Siegel, R.L., Torre, L.A., and Jemal, A. (2018). Global cancer statistics 2018: GLOBOCAN estimates of incidence and mortality worldwide for 36 cancers in 185 countries. CA Cancer J. Clin. *68*, 394–424.
3. Uno, Y. (2019). Prevention of gastric cancer by Helicobacter pylori eradication: A review from Japan. Cancer Med. *8*, 3992–4000.
4. Sun, W., and Yan, L. (2016). Gastric cancer: current and evolving treatment landscape. Chin. J. Cancer *35*, 83.
5. Zong, L., Abe, M., Seto, Y., and Ji, J. (2016). The challenge of screening for early gastric cancer in China. Lancet *388*, 2606.
6. Ransohoff, J.D., Wei, Y., and Khavari, P.A. (2018). The functions and unique features of long intergenic non-coding RNA. Nat. Rev. Mol. Cell Biol. *19*, 143–157.
7. Uszczynska-Ratajczak, B., Lagarde, J., Frankish, A., Guigó, R., and Johnson, R. (2018). Towards a complete map of the human long non-coding RNA transcriptome. Nat. Rev. Genet. *19*, 535–548.
8. Cabili, M.N., Trapnell, C., Goff, L., Koziol, M., Tazon-Vega, B., Regev, A., and Rinn, J.L. (2011). Integrative annotation of human large intergenic noncoding RNAs reveals global properties and specific subclasses. Genes Dev. *25*, 1915–1927.
9. Tan, C., Cao, J., Chen, L., Xi, X., Wang, S., Zhu, Y., Yang, L., Ma, L., Wang, D., Yin, J., et al. (2019). Noncoding RNAs Serve as Diagnosis and Prognosis Biomarkers for Hepatocellular Carcinoma. Clin. Chem. *65*, 905–915.
10. Hoefel, G., Tay, H., and Foster, P. (2019). MicroRNAs in Lung Diseases. Chest *156*, 991–1000.
11. Pichler, M., Rodriguez-Aguayo, C., Nam, S.Y., Dragomir, M.P., Bayraktar, R., Anfossi, S., Knutsen, E., Ivan, C., Fuentes-Mattei, E., Lee, S.K., et al. (2020). Therapeutic potential of FLANC, a novel primate-specific long non-coding RNA in colorectal cancer. Gut *69*, 1818–1831.
12. Wang, S., Zuo, H., Jin, J., Lv, W., Xu, Z., Fan, Y., Zhang, J., and Zuo, B. (2019). Long noncoding RNA Neat1 modulates myogenesis by recruiting Ezh2. Cell Death Dis. *10*, 505.
13. Klingenberg, M., Groß, M., Goyal, A., Polycarpou-Schwarz, M., Miersch, T., Ernst, A.S., Leupold, J., Patil, N., Warnken, U., Allgayer, H., et al. (2018). The Long Noncoding RNA Cancer Susceptibility 9 and RNA Binding Protein Heterogeneous Nuclear Ribonucleoprotein L Form a Complex and Coregulate Genes Linked to AKT Signaling. Hepatology *68*, 1817–1832.
14. Qu, L., Wang, Z.L., Chen, Q., Li, Y.M., He, H.W., Hsieh, J.J., Xue, S., Wu, Z.J., Liu, B., Tang, H., et al. (2018). Prognostic Value of a Long Non-coding RNA Signature in Localized Clear Cell Renal Cell Carcinoma. Eur. Urol. *74*, 756–763.
15. Chen, S., Xu, H., Hu, F., and Wang, T. (2020). Identification of Key Players Involved in $CoCl_2$ Hypoxia Induced Pulmonary Artery Hypertension *in vitro*. Front. Genet. *11*, 232.
16. Wang, L., Park, H.J., Dasari, S., Wang, S., Kocher, J.P., and Li, W. (2013). CPAT: Coding-Potential Assessment Tool using an alignment-free logistic regression model. Nucleic Acids Res. *41*, e74.
17. Kang, Y.J., Yang, D.C., Kong, L., Hou, M., Meng, Y.Q., Wei, L., and Gao, G. (2017). CPC2: a fast and accurate coding potential calculator based on sequence intrinsic features. Nucleic Acids Res. *45* (W1), W12–W16.
18. Qi, F., Liu, X., Wu, H., Yu, X., Wei, C., Huang, X., Ji, G., Nie, F., and Wang, K. (2017). Long noncoding AGAP2-AS1 is activated by SP1 and promotes cell proliferation and invasion in gastric cancer. J. Hematol. Oncol. *10*, 48.
19. Rahl, P.B., Lin, C.Y., Seila, A.C., Flynn, R.A., McCuine, S., Burge, C.B., Sharp, P.A., and Young, R.A. (2010). c-Myc regulates transcriptional pause release. Cell *141*, 432–445.
20. Kwak, M.K., Lee, H.J., Hur, K., Park, D.J., Lee, H.S., Kim, W.H., Lee, K.U., Choe, K.J., Guilford, P., and Yang, H.K. (2008). Expression of Krüppel-like factor 5 in human gastric carcinomas. J. Cancer Res. Clin. Oncol. *134*, 163–167.
21. Zhang, L., Wu, Y., Wu, J., Zhou, M., Li, D., Wan, X., Jin, F., Wang, Y., Lin, W., Zha, X., and Liu, Y. (2020). KLF5-mediated COX2 upregulation contributes to tumorigenesis driven by PTEN deficiency. Cell. Signal. *75*, 109767.
22. Xu, T.P., Ma, P., Wang, W.Y., Shuai, Y., Wang, Y.F., Yu, T., Xia, R., and Shu, Y.Q. (2019). KLF5 and MYC modulated LINC00346 contributes to gastric cancer progression through acting as a competing endogeous RNA and indicates poor outcome. Cell Death Differ. *26*, 2179–2193.
23. Busby, M., Hallett, M.T., and Plante, I. (2018). The Complex Subtype-Dependent Role of Connexin 43 (GJA1) in Breast Cancer. Int. J. Mol. Sci. *19*, 693.
24. Bonacquisti, E.E., and Nguyen, J. (2019). Connexin 43 (Cx43) in cancer: Implications for therapeutic approaches via gap junctions. Cancer Lett. *442*, 439–444.
25. Zhang, E., Han, L., Yin, D., He, X., Hong, L., Si, X., Qiu, M., Xu, T., De, W., Xu, L., et al. (2017). H3K27 acetylation activated-long non-coding RNA CCAT1 affects cell proliferation and migration by regulating SPRY4 and HOXB13 expression in esophageal squamous cell carcinoma. Nucleic Acids Res. *45*, 3086–3101.
26. Wang, Z., Yang, B., Zhang, M., Guo, W., Wu, Z., Wang, Y., Jia, L., Li, S., Xie, W., and Yang, D.; Cancer Genome Atlas Research Network (2018). lncRNA Epigenetic Landscape Analysis Identifies EPIC1 as an Oncogenic lncRNA that Interacts with MYC and Promotes Cell-Cycle Progression in Cancer. Cancer Cell *33*, 706–720.e9.
27. Margueron, R., and Reinberg, D. (2011). The Polycomb complex PRC2 and its mark in life. Nature *469*, 343–349.
28. Kim, K.H., and Roberts, C.W. (2016). Targeting EZH2 in cancer. Nat. Med. *22*, 128–134.

29. Emran, A.A., Chatterjee, A., Rodger, E.J., Tiffen, J.C., Gallagher, S.J., Eccles, M.R., and Hersey, P. (2019). Targeting DNA Methylation and EZH2 Activity to Overcome Melanoma Resistance to Immunotherapy. Trends Immunol. *40*, 328–344.

30. Ler, L.D., Ghosh, S., Chai, X., Thike, A.A., Heng, H.L., Siew, E.Y., Dey, S., Koh, L.K., Lim, J.Q., Lim, W.K., et al. (2017). Loss of tumor suppressor KDM6A amplifies PRC2-regulated transcriptional repression in bladder cancer and can be targeted through inhibition of EZH2. Sci. Transl. Med. *9*, eaai8312.

31. Wan, L., Xu, K., Wei, Y., Zhang, J., Han, T., Fry, C., Zhang, Z., Wang, Y.V., Huang, L., Yuan, M., et al. (2018). Phosphorylation of EZH2 by AMPK Suppresses PRC2 Methyltransferase Activity and Oncogenic Function. Mol. Cell *69*, 279–291.e5.

32. Gan, L., Xu, M., Hua, R., Tan, C., Zhang, J., Gong, Y., Wu, Z., Weng, W., Sheng, W., and Guo, W. (2018). The polycomb group protein EZH2 induces epithelial-mesenchymal transition and pluripotent phenotype of gastric cancer cells by binding to PTEN promoter. J. Hematol. Oncol. *11*, 9.

33. Xu, J., Meng, Q., Li, X., Yang, H., Xu, J., Gao, N., Sun, H., Wu, S., Familiari, G., Relucenti, M., et al. (2019). Long Noncoding RNA MIR17HG Promotes Colorectal Cancer Progression via miR-17-5p. Cancer Res. *79*, 4882–4895.

34. Li, N., Yang, G., Luo, L., Ling, L., Wang, X., Shi, L., Lan, J., Jia, X., Zhang, Q., Long, Z., et al. (2020). LncRNA THAP9-AS1 promotes pancreatic ductal adenocarcinoma growth and leads to a poor clinical outcome via sponging miR-484 and interacting with YAP. Clin. Cancer Res. *26*, 1736–1748.

35. Xia, B., Lin, M., Dong, W., Chen, H., Li, B., Zhang, X., Hou, Y., and Lou, G. (2018). Upregulation of miR-874-3p and miR-874-5p inhibits epithelial ovarian cancer malignancy via SIK2. J. Biochem. Mol. Toxicol. *32*, e22168.

36. Wang, X., Li, L., Xiao, W., and Xu, Q. (2020). Plasma microRNA-1207-5p as a Potential Biomarker for Diagnosis and Prognosis of Colorectal Cancer. Clin. Lab. *66*, https://doi.org/10.7754/Clin.Lab.2020.191269.

37. Koo, K.H., and Kwon, H. (2018). MicroRNA miR-4779 suppresses tumor growth by inducing apoptosis and cell cycle arrest through direct targeting of PAK2 and CCND3. Cell Death Dis. *9*, 77.

38. Chen, L., Lü, M.H., Zhang, D., Hao, N.B., Fan, Y.H., Wu, Y.Y., Wang, S.M., Xie, R., Fang, D.C., Zhang, H., et al. (2014). miR-1207-5p and miR-1266 suppress gastric cancer growth and invasion by targeting telomerase reverse transcriptase. Cell Death Dis. *5*, e1034.

39. You, L., Wang, H., Yang, G., Zhao, F., Zhang, J., Liu, Z., Zhang, T., Liang, Z., Liu, C., and Zhao, Y. (2018). Gemcitabine exhibits a suppressive effect on pancreatic cancer cell growth by regulating processing of PVT1 to miR1207. Mol. Oncol. *12*, 2147–2164.

40. Luo, Y., Kishi, S., Sasaki, T., Ohmori, H., Fujiwara-Tani, R., Mori, S., Goto, K., Nishiguchi, Y., Mori, T., Kawahara, I., et al. (2020). Targeting claudin-4 enhances chemosensitivity in breast cancer. Cancer Sci. *111*, 1840–1850.

41. Lin, C.H., Li, H.Y., Liu, Y.P., Kuo, P.F., Wang, W.C., Lin, F.C., Chang, W.L., Sheu, B.S., Wang, Y.C., Hung, W.C., et al. (2019). High-CLDN4 ESCC cells harbor stem-like properties and indicate for poor concurrent chemoradiation therapy response in esophageal squamous cell carcinoma. Ther. Adv. Med. Oncol. *11*, 1758835919875324.

42. Sasaki, T., Fujiwara-Tani, R., Kishi, S., Mori, S., Luo, Y., Ohmori, H., Kawahara, I., Goto, K., Nishiguchi, Y., Mori, T., et al. (2019). Targeting claudin-4 enhances chemosensitivity of pancreatic ductal carcinomas. Cancer Med. *8*, 6700–6708.

43. Kopp, F., and Mendell, J.T. (2018). Functional Classification and Experimental Dissection of Long Noncoding RNAs. Cell *172*, 393–407.

44. Zhu, H., Guo, J., Shen, Y., Dong, W., Gao, H., Miao, Y., Li, C., and Zhang, Y. (2018). Functions and Mechanisms of Tumor Necrosis Factor-α and Noncoding RNAs in Bone-Invasive Pituitary Adenomas. Clin. Cancer Res. *24*, 5757–5766.

45. Dragomir, M.P., Kopetz, S., Ajani, J.A., and Calin, G.A. (2020). Non-coding RNAs in GI cancers: from cancer hallmarks to clinical utility. Gut *69*, 748–763.

46. Liu, H.T., Liu, S., Liu, L., Ma, R.R., and Gao, P. (2018). EGR1-Mediated Transcription of lncRNA-HNF1A-AS1 Promotes Cell-Cycle Progression in Gastric Cancer. Cancer Res. *78*, 5877–5890.

47. Wang, C., Tan, C., Wen, Y., Zhang, D., Li, G., Chang, L., Su, J., and Wang, X. (2019). FOXP1-induced lncRNA CLRN1-AS1 acts as a tumor suppressor in pituitary prolactinoma by repressing the autophagy via inactivating Wnt/β-catenin signaling pathway. Cell Death Dis. *10*, 499.

48. Wang, M., Mao, C., Ouyang, L., Liu, Y., Lai, W., Liu, N., Shi, Y., Chen, L., Xiao, D., Yu, F., et al. (2019). Long noncoding RNA LINC00336 inhibits ferroptosis in lung cancer by functioning as a competing endogenous RNA. Cell Death Differ. *26*, 2329–2343.

49. Wu, X.S., Wang, F., Li, H.F., Hu, Y.P., Jiang, L., Zhang, F., Li, M.L., Wang, X.A., Jin, Y.P., Zhang, Y.J., et al. (2017). LncRNA-PAGBC acts as a microRNA sponge and promotes gallbladder tumorigenesis. EMBO Rep. *18*, 1837–1853.

50. Chen, J., Yu, Y., Li, H., Hu, Q., Chen, X., He, Y., Xue, C., Ren, F., Ren, Z., Li, J., et al. (2019). Long non-coding RNA PVT1 promotes tumor progression by regulating the miR-143/HK2 axis in gallbladder cancer. Mol. Cancer *18*, 33.

51. Huang, P., Huang, F.Z., Liu, H.Z., Zhang, T.Y., Yang, M.S., and Sun, C.Z. (2019). LncRNA MEG3 functions as a ceRNA in regulating hepatic lipogenesis by competitively binding to miR-21 with LRP6. Metabolism *94*, 1–8.

52. Humphries, B., Wang, Z., and Yang, C. (2019). MicroRNA Regulation of Epigenetic Modifiers in Breast Cancer. Cancers (Basel) *11*, 897.

53. Wang, X., Liang, Q., Zhang, L., Gou, H., Li, Z., Chen, H., Dong, Y., Ji, J., and Yu, J. (2019). C8orf76 Promotes Gastric Tumorigenicity and Metastasis by Directly Inducing lncRNA DUSP5P1 and Associates with Patient Outcomes. Clin. Cancer Res. *25*, 3128–3140.

OMTN, Volume *22*

Supplemental Information

BTEB2-Activated lncRNA TSPEAR-AS2 Drives GC Progression through Suppressing GJA1 Expression and Upregulating CLDN4 Expression

Zhong-Hua Ma, You Shuai, Xiang-Yu Gao, Yan Yan, Ke-Ming Wang, Xian-Zi Wen, and Jia-Fu Ji

Figure S1

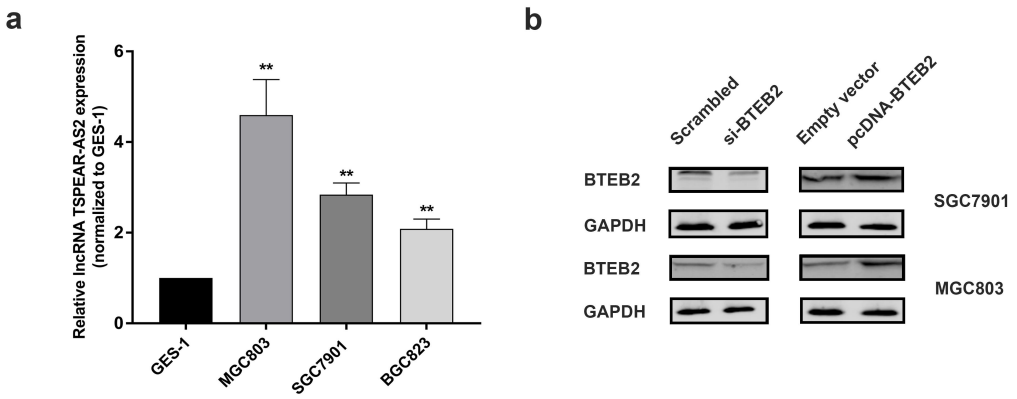

Figure S1 Relative expression level of lncRNA TSPEAR-AS2 in GC cells and the alteration of BTEB2 protein level in GC cell with BTEB2 knockdown or overexpression.

a Relative expression level of lncRNA TSPEAR-AS2 in GC at cellular level.

b BTEB2 level was detected in GC cells with BTEB2 knockdown or overexpression using western blot assays in SGC7901 and MGC803 cells.

Figure S2

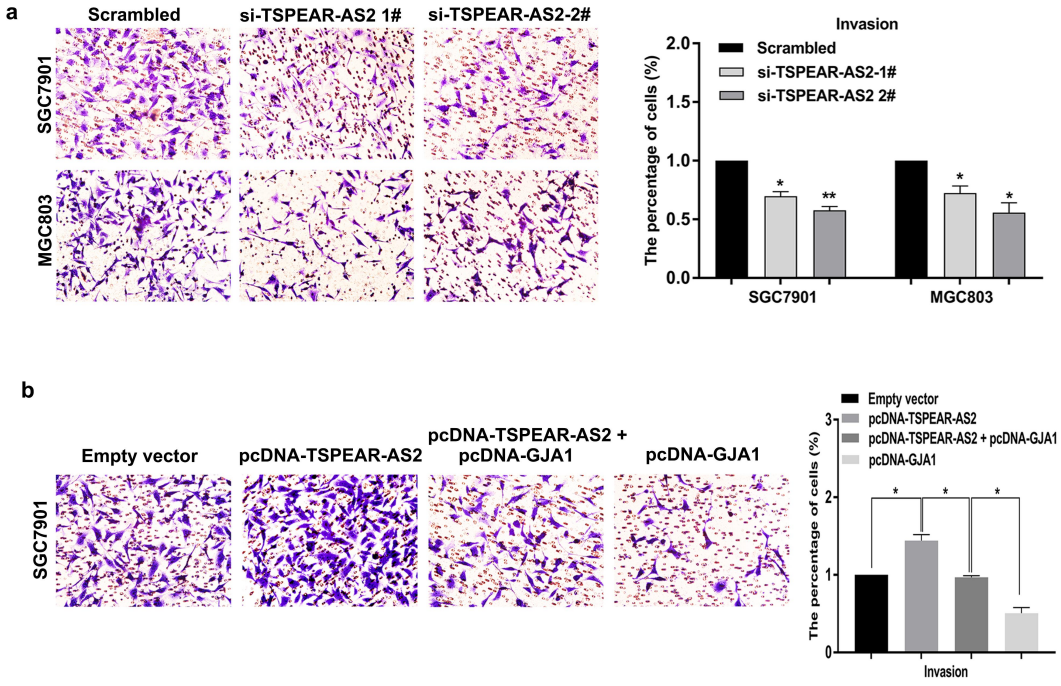

Figure S2 The involvement of GJA1 in TSPEAR-AS2-mediated GC cell invasion.

a The impact of TSPEAR-AS2 on GC cell invasion.

b GJA1 overexpression can partly reverse the promotion effects on GC cell invasion mediated by TSPEAR-AS2 overexpression. *$p < 0.05$, **$p < 0.01$.

Figure S3

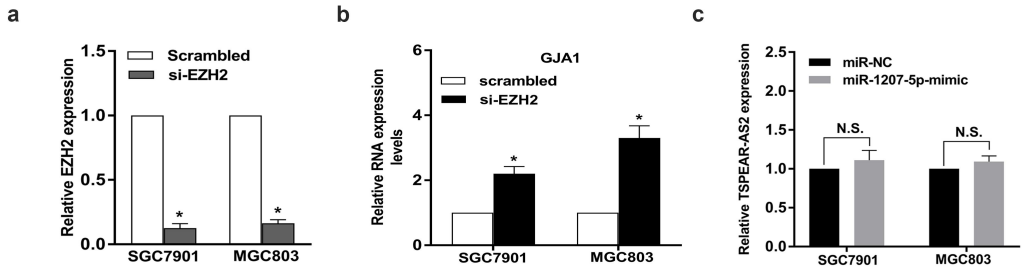

Figure S3 The impact of EZH2 depletion on GJA1 level in GC cells and the effects of miR-1207-5p on TSPEAR-AS2 regulation in GC cells.

a The knockdown efficacy of EZH2 siRNAs in GC cells.

b The expression of GJA1 in GC cells with EZH2 knockdown was analyzed by qRT-PCR assays.

c The effects of miR-1207-5p on the regulation of TSPEAR-AS2 in GC cells. *$p < 0.05$, **$p < 0.01$.

Table S1. Primers for qRT-PCR, siRNAs oligonucleotides and the company for antibody.

Primers used for qRT-PCR	
GAPDH-F	GCTCTCTGCTCCTCCTGTTC
GAPDH-R	ACGACCAAATCCGTTGACTC
CLDN4-F	AGTGGATGGACGGGTTTAGA
CLDN4-R	ACCCTCCCAGGCTCATTAGT
BTEB2-F	CTTCCACAACAGGCCACTTACTT
BTEB2-R	AGAAGCAATTGTAGCAGCATAGGA
EZH2-F	TGCACATCCTGACTTCTGTG
EZH2-R	AAGGGCATTCACCAACTCC
GJA1-F	TGTCCCTGGCCTTGAATATC
GJA1-R	GTGAGGAGCAGCCATTGAA
siRNAs oligonucleotides	
TSPEAR-AS2 1#	GGAUAAAGCCUCAAGUCCUGCAACU
TSPEAR-AS2 2#	GAGAGGAUGGCAUGGGUGACACGCA
TSPEAR-AS2 3#	GCGGCUCCUGUGUGCUUUGAAGUUU
si-EZH2	CGGCUUCCCAAUAACAGUATT
si-BTEB2	GCAGACUGCAGUGAAACAA
Antibody	**Company**
GAPDH	Cell Signaling Technology
GJA1	Abcam
IgG	Millipore
EZH2	Millipore
SUZ12	Millipore
AGO2	Millipore
CLDN4	Abcam
H3K27me3	Abcam

Supplementary Methods

Flow cytometric analysis

For apoptosis analysis, we purchased a FITC-Annexin V kit from BD Biosciences and stained GC cells with both FITC-Annexin V and PI. Then, a flow cytometer (FACScan; BD Biosciences) equipped with a CellQuest software (BD Biosciences) was used to analyze cells, which can be classified into viable cells, dead cells, early apoptotic cells, and late apoptotic cells.

RNA-expression data retrieval and analysis

Gastric cancer expression data were downloaded from the TCGA and GEO dataset. The datasets from TCGA, GSE66229, GSE65801 and GSE54397 were analyzed in this study. The BAM files and normalized probe-level intensity files were downloaded from TCGA and GEO databases, respectively. For multiple probes corresponding to a gene, the average signal generate lncRNAs. Download the probe sequences from GEO or the microarray manufacturer and reannotate probes by bowtie according to GENCODE Release 19 annotation.

RNA extraction and quantitative RT-PCR assays

Total RNA was extracted from tissues or cultured cells using TRIzol reagent (Invitrogen) according to the manufacturer's instructions. For quantification of RNA expression, cDNAs were synthesized using the PrimeScript RT Reagent Kit (TaKaRa). Real-time PCR assays were performed in triplicate with an Applied Biosystems Prism

7500 FAST Sequence Detection System using SYBR Premix Ex Taq (Takara). Human GAPDH was used as endogenous controls. RNA expression levels were investigated using the 7500 FAST System. The primers are summarized in **Table S1.**

Cell transfection

A DNA Midiprep kit (Qiagen, Hilden, Germany) was applied to manufacture the plasmid vectors for transfection. Three individual TSPEAR-AS2 siRNAs, miR-1207-5p mimics, miR-1207-5p inhibitor and scrambled negative control were obtained from Invitrogen. According to the manufacturer's instructions, GC cell lines and HEK-293T cells were transfected with siRNAs and plasmid vectors using Lipofectamine 3000 (Invitrogen). Stable knockdown of TSPEAR-AS2 level in GC cells was conducted by lenti-virus-mediated shRNA targeting TSPEAR-AS2. The sequences of these synthesized oligonucleotides for RNA interference (RNAi) are listed in **Table S1.**

Cell proliferation assays

A cell proliferation Reagent Kit I (MTT, Roche Applied Science) was used to test cell viability of GC cells with TSPEAR-AS2 knockdown or overexpression. The optical density 490 nm (OD490) was measured using a microplate reader. The other examinations of cell viability were conducted in GC cells using Cell Counting Kit-8 (CCK8; Beyotime Institute of Biotechnology, Shanghai, China) The optical density 450 nm (OD450) was measured using a microplate reader. For colony-formation

assays, cells were seeded in 6-well plates and grown for 10 days. We fixed cells with methanol and washed fixed cells with phosphate buffer saline (PBS). Then, 0.1% crystal violet (Sigma-Aldrich) was used to stain fixed cells, and the colony formation was determined by counting the number of stained colonies. The experiments were independently repeated three times.

Transwell assays

Cells were plated into the top chamber independent pathologists in migration assay, and cells were into the top chamber precoated with Matrigel in invasion assays. DMEM or RPMI1640 supplemented with 10% FBS were used to fill the bottom chamber. After incubation for 24-48 h, the cells were stained with 0.1% crystal violet for 30 min. Finally, microscope was used to calculate the number of migrated and invaded cells on the lower surface of the membrane.

Animal experiments

Four-week male BALB/c nude mice were kept in the specific pathogen-free condition. For the xenotransplantation mouse model, GC cells stably transfected sh-TSPEAR-AS2 or sh-Control were harvested and transplanted subcutaneously to either side of each mouse. The tumor volumes were calculated using the following equation: Volume = length × width × width × 0.5. Finally, the tumor weights were tested and recorded. All the mice were euthanized via CO2 asphyxiation. This study was conducted in strict accordance with the Guide for the care and Use of Laboratory

Animals of NIH. Animal protocols were approved by the Committee on the Ethics of Animal Experiments of the Nanjing Medical University. All institutional and national guidelines for the care and use of laboratory animals were followed.

RNA immunoprecipitation (RIP)

EZMagna RIP Kit (Millipore) was selected to perform RIP assays in SGC7901 and MGC803 cells. Cells lysates were prepared with complete RIP lysis buffer and followed by incubation with magnetic beads conjugated with antibodies at 4°C. Finally, the beads were washed using wash buffer, and then incubated with Proteinase K. The purified RNA was subjected to qRT-PCR assays.

Chromatin immunoprecipitation assays

EZ-ChIP Kit (Millipore, Billerica, MA, USA) was used to conduct ChIP assays in accordance with the instruction of manufacturer. SGC7901 and MGC803 cells were treated with formaldehyde and incubated for 10 min to generate DNA-protein cross-links. Anti-EZH2 and anti-H3K27me3 antibodies (Millipore) were used to immunoprecipitate chromatin fragments. Finally, qRT-PCR assays were performed to analyze the precipitated chromatin DNA.

Subcellular fractionation location and FISH assay

Based on the manufacturer's instructions, we used PAIRS Kit (Cat. AM1921, Invitrogen, CA, USA) to separate the nuclear and cytosolic portion in SGC7901 and

MGC803 cells. For FISH assay, cells were firstly fixed in 4% formaldehyde for 15 min. Fixed cells were washed with PBS and followed by treatment with pepsin (1% in 10 mmol/L HCl). Subsequently, 70%, 90%, and 100% ethanol was used for dehydration. The air-dried cells were incubated with 40 nmol/L FISH probe in hybridization buffer (100 mg/mL dextran sulfate, 10% formamide in 2× SSC) at 80°C for 2 min. Hybridization was performed at 55°C for 2 h, and the slide was washed and dehydrated. RNA FISH probes were designed and synthesized by Bogu Co, Ltd. The images were collected by using Olympus Fluoview laser scanning confocal microscope.

Prognostic analysis

Firstly, launch the http://kmplot.com/analysis/ website. Then, select module titled Start KM plotter for gastric cancer. Subsequently, enter the gene symbol and select suitable methods to split patients. Finally, click the button of draw Kaplan-Meier plot.

5-Ethynyl-2-deoxyuridine (EdU) Staining Assay

The proliferative abilities of GC cells were assessed through EdU labeling/detection kit (Ribobio, Guangzhou, China) based on the instructions of the manufacturer. The cells were cultured in Edu labeling medium, with incubation for 2 h at 37 °C under 5 % CO2. 4 % paraformaldehyde was used to fix the treated cells for 30 minutes, which were subsequently processed with 0.5 % Triton X-100 for 20 min at room temperature. After washing in PBS, the fixed cells were treated with anti-Edu working

solution at 25 °C for 30 min and subsequently processed with 0.5 % Triton X-100 for 20 min at room temperature. Next, Hoechst 33342 was used to incubate the treated cells for 30 min. Finally, fluorescent microscope was implicated for cell observation and the ratio of EdU positive cells were calculated.

Transcriptome sequencing and Data analysis

Total RNA from the SGC7901 cells with TSPEAR-AS2 knockdown and control SGC7901 cells were isolated using RNeasy mini kit (Qiagen, Germany). Paired-end libraries were synthesized by using the TruSeq RNA Sample Preparation Kit (Illumina, USA) following TruSeq RNA Sample Preparation Guide. Briefly, The poly-A containing mRNA molecules were purified using poly-T oligo-attached magnetic beads. Purified libraries were quantified by Qubit 2.0Fluorometer (Life Technologies, USA) and validated by Agilent 2100 bioanalyzer (Agilent Technologies, USA) to confirm the insert size and calculate the mole concentration. Cluster was generated by cBot with the library diluted to 10 pM and then were sequenced on the Illumina HiSeq X-ten (Illumina, USA). The library construction and sequencing was performed at Shanghai Biotechnology Corporation. Hisat2 (version:2.0.4) was used to map the cleaned reads to the human GRCh38 reference genome with two mismatches[1]. Then ,we ran Stringti (version:1.3.0) with a reference annotation to generate FPKM values for known gene models[2, 3].

References:

1. Kim D, Langmead B, Salzberg SL. HISAT: a fast spliced aligner with low memory requirements. Nat Methods 2015, 12(4):357-360.

2. Pertea M, Pertea GM, Antonescu CM, Chang TC, Mendell JT, et al. StringTie enables improved reconstruction of a transcriptome from RNA-seq reads. Nat Biotechnol 2015, 33(3):290-295.

3. Pertea M, Kim D, Pertea GM, Leek JT, Salzberg SL. Transcript-level expression analysis of RNA-seq experiments with HISAT, StringTie and Ballgown. Nat Protoc 2016, 11(9):1650-1667.